Short communication

Organic thin film transistors as selective sensing platforms for Hg^{2+} ions and the amino acid cysteine

Mohan Ramesh [b], Hong-Cheu Lin [b,**], Chih-Wei Chu [a,c,*]

[a] Research Center for Applied Sciences, Academia Sinica, Taipei 115, Taiwan, ROC
[b] Department of Materials Science and Engineering, National Chiao Tung University, Hsinchu 300, Taiwan, ROC
[c] Department of Photonics, National Chiao Tung University, Hsinchu 300, Taiwan, ROC

ABSTRACT

In this short communication we report a sensor for divalent mercuric (Hg^{2+}) ions that we constructed from a perylene bisimide (PBI)-based organic thin film transistor. We improved the performance of the n-channel device by positioning N,N′-dioctyl-3,4,9,10-perylenedicarboximide between the dielectric and the active layer (PBI), increasing the electron mobility (μ) from 0.002 to $0.25 \pm 0.04 \ cm^2 \ V^{-1} \ s^{-1}$ and enhancing the on/off ratio (I_{on}/I_{off}) by two orders of magnitude (from 10^2 to 10^4). Based on a "thymine–Hg^{2+}–thymine" mechanism and monitoring the shift in the threshold voltage (V_{th}), we used this transistor to discriminate Hg^{2+} ions from mixed ion solutions and it extended to different concentration Hg^{2+} solutions (from 50 to 350 μM). By monitoring the shifts in drain current (I_{DS}) and V_{th}, we also used this bilayer device as a sensor for cysteine, a thiol-containing amino acid; the selective detection of cysteine was accompanied by a red shift in the fluorescence maximum of PBI, from 532 to 537 nm.

© 2012 Elsevier B.V. All rights reserved.

1. Introduction

Heavy metals are environmental toxins that can accumulate in human organs without degradation (Jarup, 2003). Accumulated heavy metals (mercury, lead, cadmium) can cause several illnesses, including sleeplessness, carcinogenesis, mutagenesis, skin itching, memory loss, tremors, weakness, gingivitis, excitability, and teratogenesis (Blake et al., 2001). Among the heavy metals, mercury is particularly a toxic material that can damage the kidneys, brain, heart, and other organs (Tchounwou et al., 2003). Most mercury waste arises from chemical manufacturing, solid waste incineration, fossil fuel combustion, gold (Au) and coal mining, and wood pulping (Nolan and Lippard, 2008). The divalent mercuric ion (Hg^{2+}) is the most stable form of waste mercury; several techniques are available for its detection, including mass spectrometry (MS) (Tormen et al., 2011), electrode-based (Han et al., 2001), electrochemical, (Cao et al., 2009; Kong et al., 2009; Miao et al., 2009) and fluorometric (Liu, 2008; Wang and Liu, 2008; Ye and Yin, 2008) methods. On the other hand, the detection of amino acids (AAs) is important because, as constituents of proteins and enzymes, they play critical roles in most physiological processes (Shahrokhian,

2001). In particular, thiol-containing AAs [cysteine (Cys), homocysteine, glutathione (GSH)] are involved in many cellular functions and are, therefore, used as indicators of several major diseases, including HIV/AIDS, Alzheimer's, and various cancers (Refsum et al., 1988). Accordingly, there is high demand for rapid, sensitive, and selective sensing of thiol-containing AAs. At present, the detection and characterization of AAs is performed mostly using electrochemical (Vardanega and Giradet, 2009), electrode-based (Cooper et al., 1993), chromatographic (Wang et al., 2000), and spectroscopic (Lee et al., 2005) approaches. Therefore, the detection of Hg^{2+} ions and AAs have number of weaknesses such as, prolonged detection times, requiring sophisticated instrumentation, expensive instrumentation, low throughput, and require well-trained skilled operators. To overcome these limitations, we have developed three-terminal device organic thin film transistors (OTFTs) with additional advantages; detection on site, low cost, handheld portable, and user-friendly platform for the detection of Hg^{2+} ions and AAs.

Relative to current MS-based or optical detecting systems, OTFTs have several attractive features: they can be fabricated at low cost, over large areas, with mechanical flexibility; they consume low amounts of power; they can be surface-modified for the detection of a wide range of analytes; and they function with rapid analysis times (Lin et al., 1997). Not all available p- and n-type organic semiconductors are suitable for use as OTFT sensors, but modification with suitable probes–pyridine (Huang et al., 2004; Liu et al., 2011), bipyridyl (He et al., 2008; Wang and

* Corresponding author. Tel.: +886 227 826680x70; fax: +886 227 826680.
** Corresponding author. Tel.: +886 357 12121x55305; fax: +886 357 24727.
E-mail addresses: linhc@cc.nctu.edu.tw (H.-C. Lin),
gchu@gate.sinica.edu.tw (C.-W. Chu).

Wasielewski, 1997), terpyridyl (Kimura et al., 1998), phenanthroline (Yasuda et al., 2003), and thymine (T) (Ono and Togashi, 2004) ligands can improve their performance. A probe for ions and AAs detector should possess the following features: (i) the probe and the organic semiconductor should not be soluble in water; (ii) it should display OTFT behavior; and (iii) the resulting device must be stable in water under the operating conditions. Accordingly, we have employed perylene bisimide (PBI) as an active layer because it satisfies all of these conditions; in addition, it can present specific T probes that form stable T–Hg^{2+}–T base pairs and its n-channel OTFTs outperform start-of-the-art p-channel OTFTs and carbon field effect transistors (FETs) in the sensor pad (Huang et al., 2010; Lin et al., 2010; Sudibya et al., 2011; Zhang et al., 2010). PBI and its derivatives are important organic dyes that possess several attractive photochemical and photophysical properties (Sugiyasu et al., 2004); in particular, PBI derivatives are almost all insoluble in water and perform as good acceptors in OTFTs. As a result, we have developed PTCDI-C_8/PBI-based OTFTs for the detection of both Hg^{2+} ions and thiol-containing AAs. We monitored the sensitivity of these sensors toward (i) Hg^{2+} ions by observing the shift of the threshold voltage (V_{th}) and (ii) thiol-containing AAs by observing the changes in both the drain current (I_{DS}) and V_{th}. Our sensors detected Hg^{2+} ions at concentrations up to 50 μM and displayed the excellent sensitivity toward Hg^{2+} ions in mixed-ion media; it also detected thiol-containing AAs at millimolar concentrations.

2. Materials and methods

2.1. Sensor devices measurement

The materials, device fabrication procedure, and characterization are reported in the Appendix. Solutions of the various metal cations and AAs were prepared by dissolving them in deionized water at concentrations of 10^{-4} and 10^{-3} M; solutions containing pairs of metal cations were prepared by mixing solutions of the single metal ions of the same concentration (10^{-4} M) at 1:1 ratio. The sensor devices were tested by placing a drop (2 μL) of solution of the metal cation on top of the channel, air drying for 60 min, and then measuring under a N_2 atmosphere. Similarly, AA sensor devices were tested by placing a drop of solution on top of the channel, followed by air drying and then measuring under a N_2 atmosphere. Solutions of Hg^{2+} ions at various concentrations were prepared by diluting the stock solution (1 mM) to 50, 150, 250, and 350 μM; photoluminescence (PL) was measured according to a previously reported procedure (Ruan et al., 2010). The Fold (V_{th}/V_{0th}) was calculated by dividing the threshold voltage

shift in the presence of ions (V_{th}) by the threshold voltage in the absence of ions (V_{0th}).

3. Results and discussion

3.1. PBI device response

Fig. 1 displays a side view of the fabricated PTCDI-C8/PBI OTFT device. Patterning the dielectric through surface modification with CYTOP allowed selective deposition of the organic semiconductor in desirable regions. Recent reports have noted that SiOH groups trap electrons, but not holes, and can result in large gate leakage currents (Chua et al., 2005). The presence of hydroxyl groups on the top surface will result in inferior channel–dielectric interfaces, along with poor crystalline growth; OTFTs fabricated on such dielectric surfaces display undesirable device characteristics, including poor mobility, instability, and large gate leakage currents. The hydroxyl groups can not only result in remnant dipoles during the off-to-on gate swing but also interact with diffusing water molecules. Therefore, we deposited a reserve polymer layer (CYTOP) to ensure the preparation of OTFTs exhibiting stable operation and high electrical performance. We positioned the CYTOP film at the interface between the SiO_2 and the active layer. Fig. S1(a) presents the output characteristics of typical n-channel PBI transistors with various gate voltages (V_G); Fig. S1(b) plots I_{DS} with respect to V_G at a constant value of V_{DS} of 60 V. The device parameters we extracted from the monolayer were an electron mobility (μ) of 0.002 $cm^2 V^{-1} s^{-1}$, a threshold voltage (V_{th}) of 0.92 V, and an on/off ratio extending over two orders of magnitude. Using a bilayer method to improve the device performance and to impart stability, we introduced a film of PTCDI-C8 between the PBI layer and the SiO_2/CYTOP dielectric, observing tremendous changes in performance: values of μ and V_{th} increasing to 0.25 ± 0.04 $cm^2 V^{-1} s^{-1}$ and 13.21 ± 2 V, respectively, with a four-order (10^4) on/off ratio [Fig. S1(c) and (d)]. Therefore, we employed this device platform to prepare a sensor for Hg^{2+} ions.

3.2. OTFTs Hg^{2+} sensor

When employing the OTFTs as sensors for Hg^{2+} ions, we performed device measurements in terms of variations in V_{th}, rather than I_{DS}, because the former was easier to identify. In the presence of Hg^{2+} ions, the value of V_{th} increased by threefold (V_{th}/V_{0th}). To discern whether this change was due to the Hg^{2+} ions or another source, we measured the device performance in the presence of doubly charged (Fe^{2+}, Mg^{2+}, Cu^{2+}, Mn^{2+}, Ba^{2+}, Sn^{2+}, Ni^{2+}, Pb^{2+})
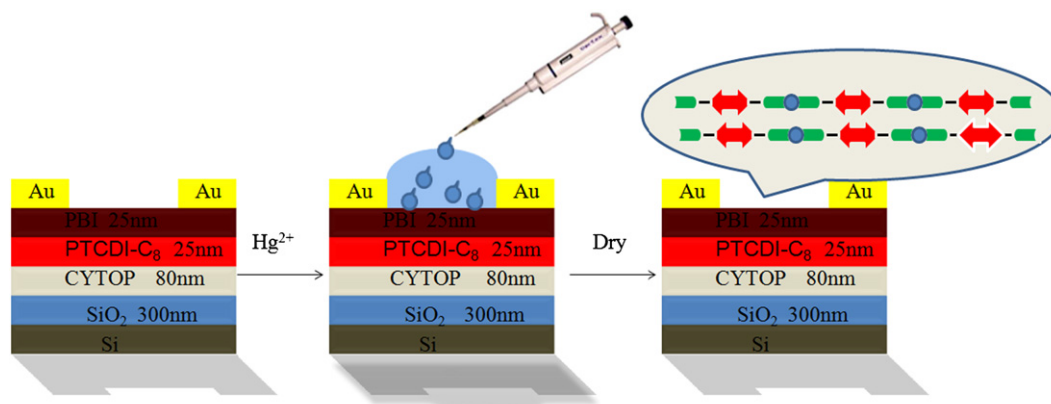

Fig. 1. Side view of the structure of the PTCDI-C_8/PBI OTFT and of the operation of the OTFT sensor in the presence of Hg(OAc)$_2$ solution.

and singly charged (Cs^+, Li^+, K^+, Na^+) ions [Fig. 2(a)]; the extracted values of V_{th}/V_{0th} for these cations ranged from 1.3 to 2.25. These differences were due to the presence of T probes in the PBI, resulting in T–Hg^{2+}–T coordination (Ruan et al., 2010). The formation of T–Hg^{2+}–T complexes trapped the Hg^{2+} ions at the interfaces of the grain boundaries of PBI [Fig. 1] and increased the overall channel resistance, thereby leading to a large change in the value of V_{th}. In contrast, the other ions (Fe^{2+}, Mg^{2+}, Cu^{2+}, Mn^{2+}, Ba^{2+}, Su^{2+}, Ni^{2+}, Pb^{2+}, Cs^+, Li^+, K^+, Na^+) were only trapped at the grain boundaries without coordination to the T ligands of the PBI. The trapped ions attracted the electrons in the channel region, thereby increasing the overall channel resistance (Khan et al., 2011; Ramesh et al., 2012). To test the selectivity of the OTFTs toward Hg^{2+} ions, we examined the effects of solutions of mixed ions.

As indicated in Fig. 2(b), we prepared mixed-ion solutions in the presence and absence of Hg^{2+} ions. The sensitivity of the probe toward the mixed Hg^{2+}-containing solutions (V_{th}/V_{0th}=ca. 4.0) was higher than that toward the solutions of single metal ions or the Hg^{2+}-free mixed ions. Furthermore, to prove that the detection was improved through T–Hg^{2+}–T coordination, we fabricated the corresponding device featuring only the PTCDI-C8 monolayer (thickness: 50 nm) and tested it with the solutions of mixed ions. Fig. S2(a) reveals that the sensitivity (V_{th}/V_{0th}) was approximately 2.5 for both

the Hg^{2+}-containing and Hg^{2+}-free solutions, presumably because of the trapping of ions at the grain boundaries. Although the device was selective toward Hg^{2+} ions at a concentration of 10^{-4} M, such performance would be inferior to that provided by current electrochemistry- and chromatography-based analytical methods. Therefore, we tested the sensitivity of this device toward Hg^{2+} solutions of lower concentrations, prepared by diluting the 1 mM stock solution; we placed a drop of each solution on top of the same device after measuring the response to the previous solution [Fig. S2(b)]. Upon increasing the concentration of the solution of Hg^{2+} ions, the value of V_{th} increased from 27.5 to 40 V; from this experiment, we found that the device could also sense Hg^{2+} ions at concentrations lower than 50 μM. We used the conventional addition method (Buck and Bakker, 1994) to calculate the limit of detection (LOD), Fig. S3(a–e); by averaging the LODs of five devices, we determined that the device could detect Hg^{2+} ions at a minimum concentration of 0.40 μM [Fig. S3(f)].

3.3. Three-terminal device as a sensor for thiol-containing AAs

After determining that the PBI-based device could be used selectively for the sensing of Hg^{2+} ions in mixed-ion solutions, we
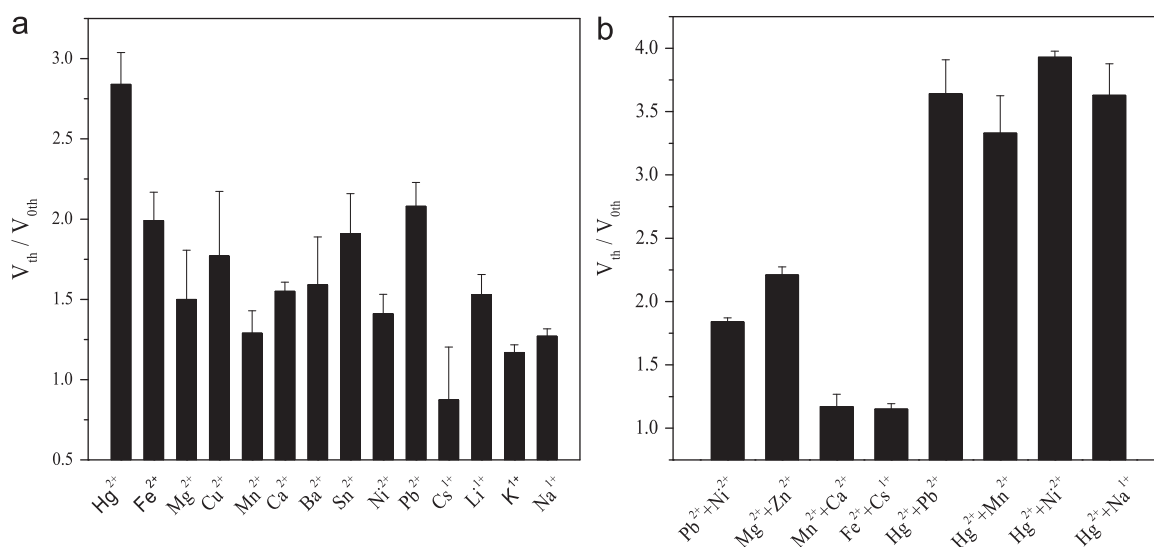
Fig. 2. (a) Threshold shifts (V_{th}/V_{0th}) of the device in the presence of various single metal ions and (b) threshold shifts (V_{th}/V_{0th}) of the device in the presence of various pairs of metal ions.
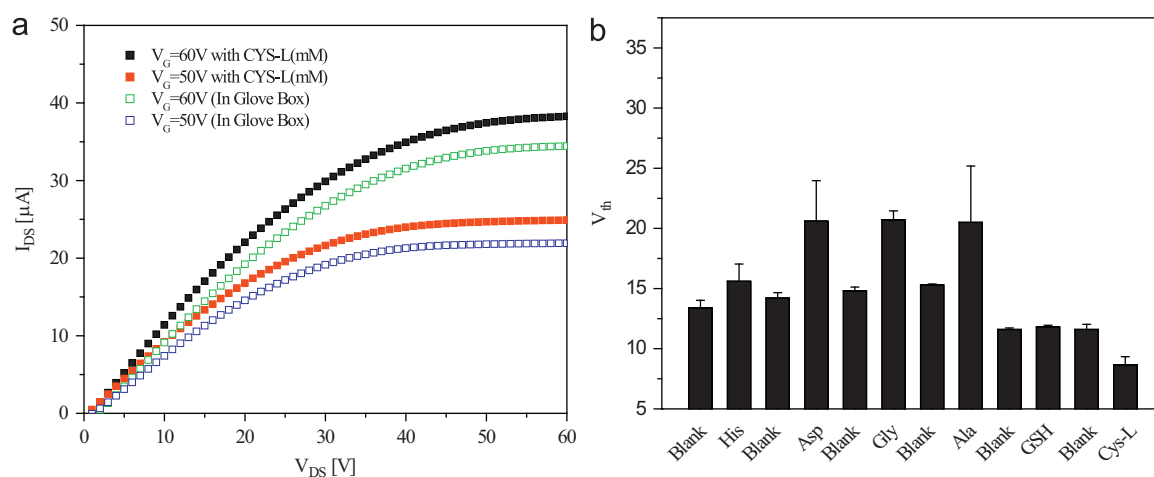
Fig. 3. (a) Changes in current (I_{DS}) of the device in the presence of Cys and (b) threshold shifts (V_{th}) of the device in the presence of various AAs.

further tested the device performance (selectivity and sensitivity) of the PTCDI-C8/PBI OTFTs as AA sensors, using an approach similar to that employed for the metal ions. For the AA sensors, we split six AAs into two categories: thiol-containing AAs (Cys, GSH) and thiol-free AAs (Ala, Asp, Gly, His); Figs. 3 and S4 display the performance of the device toward these AAs. In the presence of Cys, the value of I_{DS} increased [from 34.5 to 38.29 μA; Fig. 3(a)] and the value of V_{th} decreased [from 11.6 to 8.6 V; Fig. 3(b)]; for the other tested thiol-containing AA (GSH), the values of I_{DS} [Fig. S4(a)] and V_{th} [Fig. 3(b)] did not change as much, presumably because of the electron-donor nature of GSH (Kang et al., 1998). For the thiol-free AAs, the values of I_{DS} decreased and the values of V_{th} increased [Fig. S4(b–e) and Fig. 3(b)]. To determine the causes of these changes, we analyzed the fluorescence (PL) spectra of PBI in the presence and absence of the AAs [Fig. S4(f)]. The emission maximum of PBI in DMF/H_2O (9:1) appeared at 532 nm; adding Cys (10^{-3} M, 2 μL) to the PBI solution led to red-shifting of the fluorescence maximum to 537 nm, whereas the other AAs induced only quenching. From both the device performance and the effects on the PL spectra, it is clear that interactions occur between PBI and Cys; we are currently investigating the mechanism behind this process.

4. Conclusion

We have demonstrated that OTFTs can be used as sensors for Hg^{2+} ions and for Cys when monitoring their changes in current and threshold voltage. We converted PBI-based OTFTs into aqueous-stable OTFTs by fabricating PTCDI-C8 bilayer devices, the performance of which improved as evidenced by increases in the electron mobility (μ; from 0.002 to 0.25 $\pm$ 0.04 $cm^2\ V^{-1}\ s^{-1}$) and the on/off ratio (from 10^2 to 10^4). We employed PTCDI-C8/PBI bilayer devices in the detection of Hg^{2+} ions at a concentration of 50 μM; the detection mechanism involved T–Hg^{2+}–T coordination, which led to a dramatic shift in the value of V_{th}. Furthermore, this device could also be used for the sensitive detection of Cys, a thiol-containing AA, with the value of I_{ds} increasing from 34.5 to 38.29 μA and the value of V_{th} decreasing from 11.6 to 8.6 V; interaction with Cys led to a red shift in the fluorescence maximum of PBI from 532 to 537 nm.

Acknowledgment

Appendix A. Supporting information

Supplementary data associated with this article can be found in the online version at http://dx.doi.org/10.1016/j.bios.2012.10.050.

References

Blake, D.A., Jones, R.M., Pavlov, A.R., Darwish, I.A., Yu, H.N., 2001. Biosensors & Bioelectronics 16, 799–809.
Buck, R.P., Bakker, E., 1994. Pure and Applied Chemistry 66, 2527–2536.
Cao, R.G., Zhu, B., Li, J.J., Xu, D.S., 2009. Electrochemistry Communications 11, 1815–1818.
Chua, L., Zaumseil, J., Chang, J., Ou, E.C., Ho, P.K., Sirringhaus, H., Friend, R.H., 2005. Nature 434, 194–199.
Cooper, J.C., Hämmerle, M., Schuhmann, W., Schmidt, H.L., 1993. Biosensors & Bioelectronics 8, 65–74.
Han, S., Zhu, M., Yuan, Z., Li, X., 2001. Biosensors & Bioelectronics 16, 9–16.
He, S., Iacono, S.T., Dennis, A.E., Smith, D.W., Smith, R.C., 2008. Journal of Materials Chemistry 18, 1970–1976.
Huang, H., Wang, K., Tan, W., Zhai, Q., Zhou, L., Jin, Y., 2004. Angewandte Chemie, International Edition 43, 5635–5638.
Huang, Y., Palkar, P.V., Li, L.-J., Zhang, H., Chen, P., 2010. Biosensors & Bioelectronics 25, 1834–1837.
Jarup, L., 2003. British Medical Bulletin 68, 167–182.
Kang, S.W., Chae, H.Z., Seo, M.S., Kim, K., Baines, I.C., Rhee, S.G., 1998. Journal of Biological Chemistry 273, 6297–6302.
Khan, H.U., Jang, J., Kim, J.J., Knoll, W., 2011. Journal of the American Chemical Society 133, 2170–2176.
Kimura, M., Horai, T., Hanabusa, K., Shirai, H., 1998. Advanced Materials 10, 459–462.
Kong, R.M., Zhang, X.B., Jin, X.Y., Huan, S.Y., Shen, G.L., Yu, R.Q., 2009. Chemical Communications 37, 5633–5635.
Lee, C.S., Teng, P.F., Wong, W.L., Kwong, H.L., Chan, A.S.C., 2005. Tetrahedron 61, 7924–7930.
Lin, T.W., Kekuda, D., Chu, C.W., 2010. Biosensors & Bioelectronics 25, 2706–2710.
Lin, Y.Y., Gundlach, D.J., Nelson, S.F., Jackson, T.N., 1997. IEEE Electron Device Letters 18, 606–608.
Liu, B., 2008. Biosensors & Bioelectronics 24, 756–760.
Liu, B., Bao, Y., Wang, H., Tian, J., Bai, R., 2011. Chemical Communications 47, 1731–1733.
Miao, P., Liu, L., Li, Y., Li, G.X., 2009. Electrochemistry Communications 11, 1904–1907.
Nolan, E.M., Lippard, S.J., 2008. Chemical Reviews 108, 3443–3480.
Ono, A., Togashi, H., 2004. Angewandte Chemie, International Edition 43, 4300–4302.
Ramesh, M., Lin, H.C., Chu, C.W., 2012. Journal of Materials Chemistry 22, 16506–16513.
Refsum, H., Ueland, P.M., Nygard, O., Vollset, S.E., 1988. Annual Review of Medicine 49, 31–62.
Ruan, Y.-B., Li, A.-F., Shen, J.-S., Jiang, Y.-B., 2010. Chemical Communications 46, 4938–4940.
Shahrokhian, S., 2001. Analytical Chemistry 73, 5972–5978.
Sudibya, G.H., He, Q.G., Zhang, H., Chen, P., 2011. ACS Nano 5, 1990–1994.
Sugiyasu, K., Fujita, N., Shinkai, S., 2004. Angewandte Chemie, International Edition 43, 1229–1233.
Tchounwou, P.B., Ayensu, W.K., Ninashvili, N., Sutton, D., 2003. Environmental Toxicology 18, 149–175.
Tormen, L., Torres, D.P., Dittert, I.M., Frescura, V.L.A., Curtius, A.J., 2011. Journal of Food Composition and Analysis 24, 95–102.
Vardanega, D., Giradet, C., 2009. Chemical Physics Letters 469, 172–176.
Wang, B., Wasielewski, M.R., 1997. Journal of the American Chemical Society 119, 12–21.
Wang, J., Chtrathi, M.P., Tian, B., 2000. Analytical Chemistry 72, 5774–5778.
Wang, J., Liu, B., 2008. Chemical Communications 39, 4759–4761.
Yasuda, T., Yamaguchi, I., Yamamoto, T., 2003. Advanced Materials 15, 293–296.
Ye, B.C., Yin, B.C., 2008. Angewandte Chemie, International Edition 47, 8386–8389.
Zhang, Q., Jagannathan, L., Subramanian, V., 2010. Biosensors & Bioelectronics 25, 972–977.